Time Difference of Arrival Based Indoor Positioning System Using Visible Light Communication

SAAD MEHMOOD SHEIKH[1], HAFIZ M. ASIF[ID][4], KAAMRAN RAAHEMIFAR[2,3,4], AND FADI AL-TURJMAN[ID][5]

[1]Department of Electrical and Computer Engineering, COMSATS University Islamabad, Lahore Campus, Lahore 54000, Pakistan
[2]College of Information Sciences and Technology (IST), Data Science and Artificial Intelligence Program, Penn State University, State College, Pennsylvania, PA 16801, USA
[3]School of Optometry and Vision Science, Faculty of Science Department of Chemical Engineering, Faculty of Engineering, University of Waterloo, Waterloo, ON N2L 3G1, Canada
[4]Department of Electrical and Computer Engineering, Sultan Qaboos University, Muscat 123, Oman
[5]Artificial Intelligence Engineering Department, Research Center for AI and IoT, Near East University, Nicosia 99138, Mersin 10, Turkey

Corresponding author: Hafiz M. Asif (h.asif@squ.edu.om)

ABSTRACT Visible Light Communication (VLC) is a novel optical wireless communication technology which uses Light Emitting Diodes (LEDs) and Photodiodes for coherent detection and very-high-data rate data communication system. The stringent Line of Sight (LoS) requirement in VLC makes it very suitable for Indoor Positioning System (IPS), to be used for autonomous and smart city infrastructure. The current work aims to implement a real time IPS system using VLC link in Network Simulator (NS-3). The VLC module is implemented by modelling real-time attributes of LEDs, optical channel, and the photodiodes. The localization is carried out using trilateration schemes which measures the Received Signal Strength Indication (RSSI) and the Time Difference of Arrival (TDoA) for position estimation of the target. The project is further extended to obtain a comparative analysis between VLC link and other existing technology, Wi-Fi, as far as positioning accuracy and other important performance metrics are concerned. The simulation results show significant improvement for the VLC link over the Wi-Fi link specially for the TDoA scheme accompanied by increasing number of beacon nodes.

INDEX TERMS Visible light communication, IPS, RSSI, TDoA, trilateration or multilateration, NS-3 simulator.

I. INTRODUCTION

Since the inception of RF technologies, there has been a tremendous growth in the telecommunication sector, especially the wireless networks. However, with the increase in demand of RF spectrum, RF spectrum saturation has been observed. The interference between the communication links has also taken a toll [1]. Due to this dilemma, optical communication technologies, i.e., non-RF spectrum technologies, have gained considerable attention of data communication researchers. Amongst optical communication technologies, VLC is relatively a recent data communication that offer

The associate editor coordinating the review of this manuscript and approving it for publication was Md. Arafatur Rahman[ID].

extremely high data rate and inherent security [2]. This is because the VLC provides the best of the transmission characteristics with the minimum trade-off. Other salient features include non-penetration to walls, cost effectiveness, vast spectrum of communication, no interference with RF spectrum (430-790THz), and high resolution for localization applications [3]. The communication over a VLC link is highly secure for covert communication due to opacity hindrance because VLC signal cannot pass through walls and other opaque materials. The high transmission speed, safety, low energy consumptions and operating in restricting environments, all provide an edge to VLC over the standard Wireless communication technologies [4]. It is worth-mentioning that although VLC links are very reliable due to

the non-interference of RF signals, yet Low Density Parity Check (LDPC) codes are, in general, able to achieve the capacity-approaching performance of a myriad of communication systems. However, the present work does not take into consideration the use of LDPC codes due to the scope of the work [5], [6]. The VLC systems use LEDs to transmit wireless data over long distances and support super dense environments due to its Line-of-Sight (LoS) property [7]. This has given rise to the recent research studies with the VLC for indoor positioning system. LoS is a strict condition to compute the positioning in VLC. Standard interferences are nearly negligible in a VLC-IPS link with the only interference involved from opaque obstacles and ambient light [8]. Thus, high precision positioning system is achieved using VLC. VLC based networks have huge number of indoor applications which can be applied to make a convenient living for all. Ranging from indoor positioning to providing data networks to all the devices, VLC systems can be used for our everyday requirements like communication with our devices, wireless sensor networks, access control systems, etc.

A. PRIOR WORK AND CONTRIBUTION

Localization and positioning have become an emerging state-of-art research topic due to the increase in the demand for accurate positioning services. Numerous Positioning Applications like autonomous vehicular system, robot positioning recognition and control, Navigation services, asset and people tracking, augmented reality and immersive experiences has all given rise to the study of both indoor and outdoor localization/positioning techniques [9]. A range of indoor positioning technologies has been proposed over time, which includes Bluetooth [10], Ultra-Wide Band (UWB) [11], RFID [12], [13], Microelectromechanical Systems (MEMS) [14], WLAN [15], computer vision [16], magnetic field [17], ultrasonic waves [18], infrared signal and other indoor positioning technologies [19]–[24]. Bluetooth provides a low-powered indoor positioning system contributing to easy deployment, low power consumption, and low cost.

There are myriad types of positioning algorithms based on different metrics such as Received Signal Strength Indication (RSSI)-distance method, Time-of-Arrival positioning, wireless fingerprint positioning etc. [25], [26]. Given the channel model, the RSSI-distance method keeps track of the received signal strength (RSS) in order to estimate the position of the target. A Bluetooth-based trilateration positioning was exploited for the estimation of the target in [10]. Moreover, an extended Kalman filter approach was deployed to process the Bluetooth signals using the RSSI-distance model in [27]. This method can provide accurate localization with the dependency of precise and high intensity signal strength. However, little attention was paid to the accuracy especially in a practical test. Another work was carried out to use Back Propagation Neural Network (BPNN) in the RSSI-distance method in an attempt to improve the positioning accuracy. The proposed model did increase the accuracy at the cost of

complex data acquisition and training cost of BPNN [28]. A similar work was also reported in [29] in which an indoor VLC localization was proposed by combining deep neural network based on the Bayesian Regularization (BR-DNN) and sparse diagonal training data set. Accuracy of up to 3.40 *cm* was demonstrated using experimental set up. In [30], a relatively low-complexity TDoA-VLC system was experimentally demonstrated by making use of virtual oscillator (to reduce hardware complexity) and cubic interpolation to reduce the sampling rate. Their results produced an accuracy up to 9.2 cm using proposed hardware.

RSSI-distance was employed slightly differently in [27] as the model was preceded by Kalman filter for RSSI collection followed by curve fitting. The weighted Least Square Estimation (LSE) algorithm was used to measure accurately the position of the target. Unfortunately, Kalman filter did not turn out to be optimal because the distribution of the RSSI fluctuation noise is non-Gaussian. It is worth-revealing that Fingerprint localization also uses RSSI-based method along with neural network for position estimation. In another localization implementation [23], the dynamic implementation of the distance loss model parameters was suggested. The anchor nodes estimate these parameters in a cooperative fashion. Afterwards, any trilateration algorithm was deployed for the estimation of the target's position. This method can be used, however, it is computationally expensive.

Many attempts have been carried out in localization applications using VLC technology, for example, combination of an array of LEDs and image sensors were exploited to locate the receiver using trilateration scheme [31], [32] but the accuracy was barely achieved up to 22 *cm*. The work done in [33] makes use of the TDoA for VLC systems. However, their accuracy is limited due to static phase of the transmitted signal. Similarly, an accuracy of up to 2.4 cm was recorded based on three channel transmission method for localization as the cost of very complex receiver structure [34]. In none of the attempts, up to millimeters accuracy was achieved.

B. CONTRIBUTION

The key contribution lies in developing and VLC channel module to replace the existing RF channel. In this work, we develop a new module for VLC in Network Simulator (NS-3) using extensive modular approach in the simulator. The module is designed by modelling the mathematical equations of VLC LoS and NLoS channels. The Modelling involves simulating all the real-time parameters for the LEDs and the photodiodes along with the channel models. The developed channel is then used for localization applications mainly based on RSSI and a novel Time Difference of Arrival (TDoA) algorithms. The selected performance metrics are positioning error, the received power, and the effect of anchor nodes for evaluation. The detailed structural chart for the VLC-IPS module is shown in Fig.1. The results are compared with Wi-Fi-based real-time Experiments and the observations are drawn accordingly. Fig.2 signifies the flowchart of the NS-3 based VLC-IPS module implementing
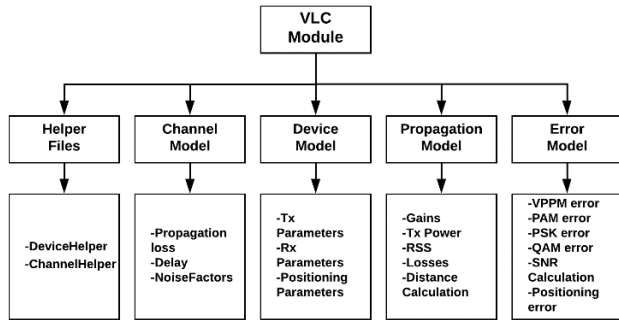
FIGURE 1. NS-3 based VLC-IPS module.

the TDoA positioning. The implementation uniqueness of our work lies in the fact that the system will be implemented on real-time simulator NS-3 which will consider all the real-time parameters to provide the most accurate results.

C. ORGANIZATION
The rest of the paper is organized as follows: Section II presents detailed discussion for the positioning techniques used in our system (RSSI and TDoA). VLC channel modelling is described in section III. Section IV explains NS-3 Fundamentals and NS-3 based TDoA Implementation. Results are presented and explained in section V. Section VI concludes the paper and elaborates future research challenges.

II. POSITIONING ALGORITHMS
Trilateration or Multi-Lateration is the analytical range estimation-based positioning scheme which is an indirect method of calculating the position and the Euclidean distance between the beacons and the unknown node through various mathematical or empirical models [35], [36]. These mathematical models include the RSSI, TDoA, Phase difference of Arrival (PDoA) and Time of Arrival (ToA). Trilateration can be implemented for large number of beacon nodes in form of simultaneous equations. This can be further extended to representing in Matrix formation for implementing in simulators and other modelling tools.

For e.g., considering distances estimates for n beacons where ($n \geq 4$), the trilateration or Multi-Lateration system can be defined as:

$$2 \begin{bmatrix} x_1 - x_n & y_1 - y_n \\ \vdots & \vdots \\ x_n - x_{n-1} & y_n - y_{n-1} \end{bmatrix} \begin{bmatrix} x_u \\ y_u \end{bmatrix}$$
$$= \begin{bmatrix} (r_1^2 - r_n^2) - (x_1^2 - x_n^2) - (y_1^2 - y_n^2) \\ \vdots \\ (r_{n-1}^2 - r_n^2) - (x_{n-1}^2 - x_n^2) - (y_{n-1}^2 - y_n^2) \end{bmatrix} \quad (1)$$

where (x_u, y_u) are the coordinates of the unknown node U, (x_i, y_i) are the coordinates of the known beacon node B_i and r_i is the Euclidean distance between the unknown node and

the beacon. The above matrix can be simplified as:

$$A^T.A.x = A^T.b \quad (2)$$

where: $A = 2 \times$ L.H.S matrix.

$$x = [x_u, y_u]^T$$
$$b = \text{R.H.S matrix}$$

The above matrix can further be simplified using various factorization methods such as Cholesky or QR factorization to accurately find the positioning of the unknown node.

A. RSSI SCHEME
The RSSI scheme requires the wireless network nodes to be in a line-of-slight connection and transmitting signals at a defined interval. Multiple beacon nodes transmit their signals and is received by the unknown node placed a certain distance [37]. The RSSI scheme approximates the received power magnitude which is transmitted over a certain distance and is affected by various factors like pathloss and interferences. The Friis Free space propagation model signifies the pathloss model for the RSSI scheme. The Model is a function of transmitted power, distance between sender-receiver, the signal wavelength and the antenna gains. Similarly, the Log Normal Shadowing (LNS) model is also used to calculate the RSS for a signal transmitted over a certain distance [38]. In this model, a pathloss exponent (γ) is used to signify the real-time effects accountable for interference and pathloss like absorption, diffraction, scattering, reflection, and material attenuation.

$$P_{rx} = P_0 - 10.\gamma.\log\left(\frac{d_{ij}}{d_0}\right) \quad (3)$$

By solving Eq. 3 for d_{ij}, P_0 and γ, the distances between the unknown and the beacon nodes can be calculated through the RSS method and finally using Eq. 1, the position can be found with maximum accuracy.

If the distance needs to be calculated for beacon nodes placed at uniform distances the pathloss model can be modified in form a Three Log Distance Propagation Loss Model. This model is best suited for beacons ($n \leq 4$) as the model is used to calculate the Received power or unknown distance with respect to three distance fields: near, middle and far, each with its own exponents as per Eq. 4.

$$L = \begin{cases} 0 & d < d_o \\ L_0 + 10.n_0 log_{10}\left(\frac{d}{d_0}\right) & d_o \leq d \leq d_1 \\ L_0 + 10.n_0 log_{10}\left(\frac{d_1}{d_0}\right) \\ \quad + 10.n_1 log_{10}\left(\frac{d}{d_1}\right) & d_1 \leq d \leq d_2 \\ L_0 + 10.n_0 log_{10}\left(\frac{d_1}{d_0}\right) \\ \quad + 10.n_1 log_{10}\left(\frac{d_2}{d_1}\right) \\ \quad + 10.n_2 log_{10}\left(\frac{d}{d_2}\right) & d_2 \leq d \end{cases} \quad (4)$$
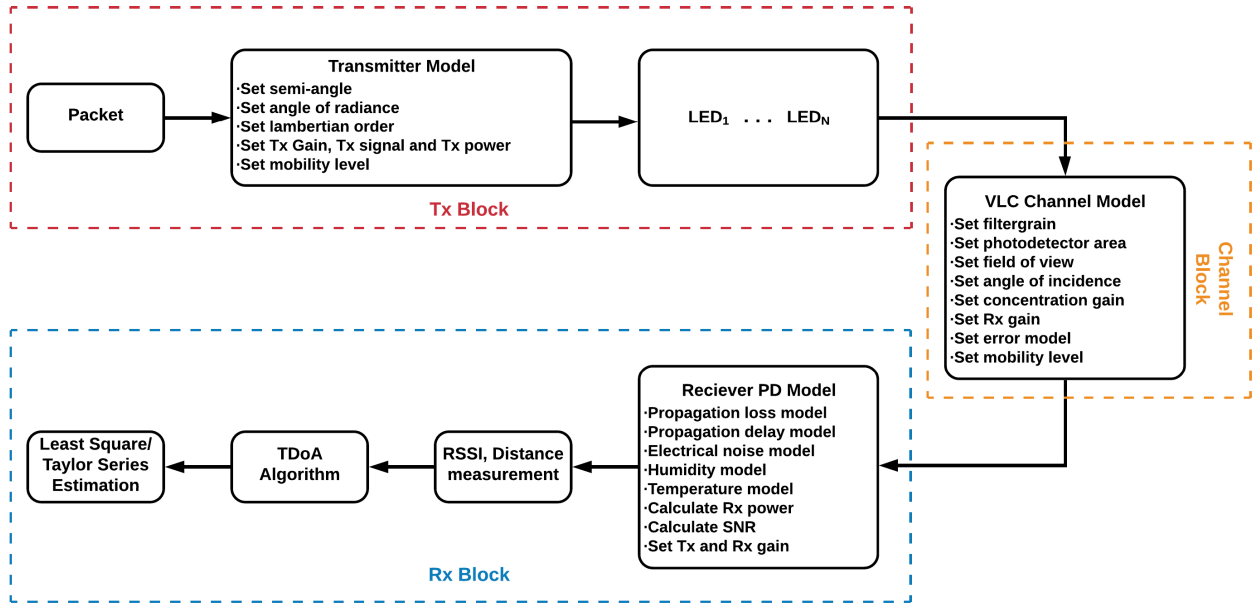
FIGURE 2. NS-3 based TDoA implementation.

where:

L = Received pathloss (dB)

d = distance (m)

d_o, d_1, d_2 = three distance fields

n_o, n_1, n_2 = pathloss distance exponents for each field.

L_o = reference pathloss (dB) = 46.67dB (Friis standard)

B. TDoA SCHEME

The TDoA algorithm makes use of the time difference of the signal being received at the unknown node. This algorithm involves the multiple beacon nodes placed and various distances and all transmitting signals at the same time. Due to various distances, the signal is received with different time delays at the receiver node. These time delays represent the phase shift of each transmitted signal and it is used to accurately pinpoint the position of the receiving node. As shown in Fig.3, the phase differences are represented by hyperbolas for each transmitted node and the intersection of these hyperbolas marks the position of the unknown node. TDoA has been used for various indoor and outdoor applications [9]. For Civil technology, it is used in mobile communication systems for positioning and localization of cell phones for their subscribers. The location of different ships and boats are estimated by using the information of their acoustic waves TDoA. For military applications, TDoA is used to estimate the position of the enemy's communication devices via the RF waves emitted.

The key advantages of using a TDoA method are 1) a single antenna per sensor and at least four sensors are required for 3-D localization. Whereas for the triangulation, an array of sensors is used for each measurement and at least two direction Finding sites are required, and 2) a very high precision and accuracy in positioning can be achieved. Similarly,
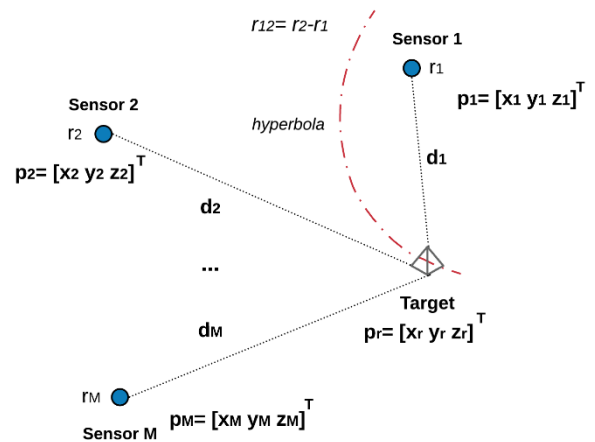

FIGURE 3. Hyperbolic definition for TDoA system.

the drawbacks for the TDoA is due to its dependency of accurate and synchronized clocks for each sensor. The TDoA accuracy depends on:

- Measurement error at the transmitter/beacons' end.
- Multipath problems for RF based Beacons.
- Timing Accuracy for the beacons

III. VLC CHANNEL MODELLING

The VLC channel model is fundamentally defined upon its both Line-of-Sight (LoS) and Non-LoS response.

$$H_{ow}(f) = H_{los} + H_{nlos} \qquad (5)$$

where:

$H_{ow}(f)$ = Total optical wireless channel response

H_{los} = channel response for LoS

H_{nlos} = channel response for NLoS

A. LoS CHANNEL RESPONSE

The channel response for LoS depends upon on various transmitter and receiver properties like, Lambertian Radiant intensity (R), maximum radiated power (Φ), Transmitted power (P_t), Effective area of Photodiode (A_{eff} (ψ)) which is further dependent on the Field of View of the Receiver signified by (ψ). The optical gain is also a major factor for the calculation of the channel response $g(\psi)$.

Hence the line-of-sight channel gain can be defined as a function of a Lambertian source of a certain DC gain, a receiver with an optical band-pass filter $T_s(\psi)$, a non-imaging concentrator placed a distance d and a radiant angle ϕ w.r.t to the transmitter position [39]. The mathematical definition is given in Eq. 6.

$$H_{los}(0) = \begin{cases} \dfrac{Ar(m+1)}{2\pi d^2}cos^m(\phi)T_s(\psi) \\ \times g(\psi)cos\psi & 0 \leq \psi \leq \psi_c \\ 0 & elsewhere \end{cases} \quad (6)$$

where:

H_{los} = channel Response for LoS.
Ar = Surface area of the photodiode.
$cos^m(\phi)$ = receiver Field of view (semiangle).
$T_s(\psi)$ = optical filter gain.
$g(\psi)$ = optical concentrator gain.
D = distance from LED to Rx point.

Using the Channel response, the received power can also be calculated as:

$$P_{r-LoS} = H_{los}(0)P_t \quad (7)$$

B. NLoS CHANNEL RESPONSE

The NLoS has much more complex response compared to the LoS since various dependencies like network scenario dimensions (in case of indoor testing), reflections from various obstacles and positioning and orientation of the transmitter and receiver all contribute to the variations in the channel response [40]. hence, the channel response can be modelled as:

$$H_{nlos} = \frac{\rho(m+1)A_{pd}}{2\pi^2 D_1^2 D_2^2}cos^m\phi_1 cos\psi_1 cos\phi_2 cos\psi_2 \quad (8)$$

where:

D_1 = distance between transmitter and point of reflection
D_2 = distance between receiver and point of reflection
ρ = Reflectivity constant
ϕ_1 = Transmitter's angle of radiance
ψ_1 = Transmitter's angle of incidence
ϕ_2 = Receiver's angle of radiance
ψ_2 = Receiver's angle of incidence

IV. NS-3 FUNDAMENTALS

The greatest advantage of a network simulator is that it diminishes the cost for the testbed analysis during commercialization as the modelling and experimentation is real-time based. There are many types of network simulators, but choice of

NS-3 is due its discreteness feature. NS-3 provides the user the edge of implementing every layer individually and discretely without altering the other layers. The NS-3 works on set of libraries, which helps the user in connecting to other type of simulators without any inconvenience. Due to its modular property, NS-3 can connect and integrate with various types of external animators, data analysis and visualization tools [41].

The choice of NS-3 is because:

- NS-3 is open source and openly accessible for researchers interested about assessing framework level deployments.
- NS-3 comprises of a set of libraries and other outside software libraries that can be combined to assess expansive systems with a variety of access technologies.
- NS-3 protocols are planned to be exceptionally similar to real-time effects of hardware devices in terms of performance, which permits for examination of expansive systems without the need to deploy the physical system.
- NS-3 simulations support real-time schedulers that allow them to interact with real systems.

NS-3 is built as a library, which can be statistically or dynamically linked to C++ main program that defines the simulation topology and starts the simulator. Another feature of NS-3 is that all the Application Programming Interface (APIs) can be exported provided APIs are programmed in Python language. This feature is scarce in other network simulators.

A. MODULAR DEFINITION OF VLC MODULE

The first objective is to model an VLC based channel in Ns-3, via mathematical modelling of its various real-time components [4], [42]. More details about VLC module implementation can be found in [4].

1) HELPER FILES

The top layer of the module known as the helper files, encloses all the implemented models. There are two wrapper files utilized in the current module. The primary file is DeviceHelper, which models the real-time characteristics and specifications of the transmitter and the receiver. The secondary is ChannelHelper file, that consists of salient features of optical channel such as losses, the propagation models and other channel effects.

2) CHANNEL MODEL

Channel model files incorporates the characteristics of the entire medium connecting the transmitter all the way to the receiver. It is worth noting that the real-time characteristics are considered (e.g., noise etc.). It also involves computation of physical propagation phenomena such as reflection, refraction etc. Other parameters include both electrical and optical bandwidth, average delay, gains at both ends and the noise distribution. For the calculation of the noise, temperature, pressure, climate conditions (light, rain, clouds etc.) are all

considered. Last but not least is the tracking of the mobility of the users while measuring the separation between them efficiently.

3) DEVICE MODEL

The device model outputs real-time results about the operation of real-time transmitter and receiver models by incorporating all the essential characteristics of the transceiver during simulation. For instance, the parameters such gains at both ends (concentrator, filter, amplification, attenuation etc.), reflection/refraction angles/semi angles, sensitivity at the receiving device, and the mobility parameters.

4) PROPAGATION MODEL

The subsequent model contains the data regarding the channel noise, temperature, bandwidth, saturation, and the channel gains and losses, which effect the real-time channel.

5) ERROR MODEL

Following model calculates the Bit Error Rate (BER), Symbol Error Rate (SER) and throughput for the various modulation schemes applied in the channel along with the positioning error through different positioning schemes.

B. NS-3 BASED TDoA IMPLEMENTATION

As per the system definition in Fig. 2, our contribution and main focus is the Rx block where the positioning algorithms are implemented. Packet transmitted contains the official positioning coordinates of the transmitters along with the Internet Message Access Protocol (IMAP) data. The transmitter model, as explained section 4.1, models all the characteristics and attributes for the array of smart LEDs. The LEDs further transmit the signal over a VLC channel simultaneously and all the real-time effects of the channel are modelled to simulate a real-time network. The signal received at the receiver end goes through the positioning process which involves the calculation of the RSSI through different pathloss model explained in section 2.1 and the distance between the receiver and each transmitter is calculated. The following signal is further processed under TDoA algorithm where the different time or arrivals of signals from each transmitter is determined and the position of the PD/receiver node is estimated using the different methods like least square estimation, Newton Raphson and Taylor series which are dependent on the number of transmitter/beacon nodes used.

In TDoA, the assumptions of stationary position and the synchronization of clocks of the beacons is necessary to avoid the Doppler effects. Hence, the phase difference or time delay of arrival is only due to the ambient interferences and positioning of the beacons which is modelled in the VLC channel [8].

C. MATHEMATICAL MODELLING FOR NS-3 BASED TDoA LOCALIZATION

The TDOA localization scenario shown in Fig.4 contains the sensor nodes transmitting signal with some delay in time and
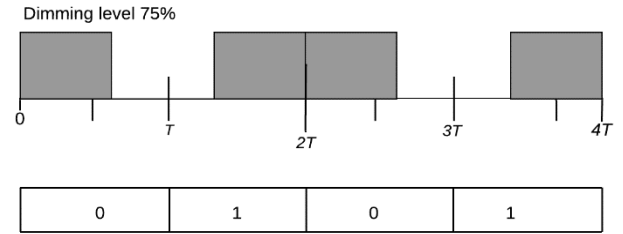

FIGURE 4. Dual operation of VPPM modulation.

frequency. The Received signal from the ith sensor can be calculated by Eq. 9:

$$y_i(t) = e^{j\alpha_i} e^{-jw_{d_i}t} s(t - \tau_i) + n(t), \quad i = 1, 2, \ldots M \quad (9)$$

where α_i is the phase due to the time of transmission of the signal and w_{d_i} is the Doppler frequency shift of the ith sensor with velocity v_i. The phase difference and Doppler frequency shift can be calculated as:

$$\alpha_i = w_c \tau_i \quad (10)$$

$$w_{d_i} = \frac{w_c v_i}{c} \quad (11)$$

Since in TDOA, the beacons are assumed to be stationary and synchronized hence the Doppler shift is considered to be zero. Therefore, the classic approach for estimating TDOA is to compute the cross correlation between signals arriving at the target node from all the sensors. The Cross correlation can be represented as:

$$R_{y_1 y_2}(\tau_{12}) = \int_0^T y_1(t) y_2(t - \tau_{12}) \, dt \quad (12)$$

The TDOA between the 1st and 2nd beacon node can found by calculating the peak of $|R_{y_1 y_2}(\tau_{12})|$. Now since we know:

$$\tau_{12} = \tau_2 - \tau_1 \quad (13)$$

Hence, we can write τ_{12} in form of its distances of d_2 and d_1 respectively, hence the above equation becomes:

$$\tau_{12} = \frac{d_2 - d_1}{c} \quad (14)$$

And

$$d_2 = d_1 + c\tau_{12} \quad (15)$$

$$d_i = ||p_i - p_T|| \quad (16)$$

$$d_i = \sqrt{(x_i - x_T)^2 + (y_i - y_T)^2 + (z_i - z_T)^2}, \\ i = 1, 2, 3, \ldots \ldots M \quad (17)$$

$$d_i^2 = (x_i - x_T)^2 + (y_i - y_T)^2 + (z_i - z_T)^2, \\ i = 1, 2, 3 \ldots \ldots M \quad (18)$$

The solution for Eq. 18 can be resolved either by Least Square linearization (at least 5 sensors) or Taylor expansion series (max 4 sensors)

1) LINEAR SQUARE LINEARIZATION

The following scheme is a modification of Eq. 1, where the distance from the 1st sensor is taken as reference and it is subtracted from distance of the ith sensor [15]. Hence the equations are formed as:

$$d_1^2 = (x_1 - x_T)^2 + (y_1 - y_T)^2 + (z_1 - z_T)^2 \quad (19)$$

$$d_i^2 = (d_1 + c\tau_{1i})^2 = (x_1 - x_T)^2 + (y_1 - y_T)^2 + (z_1 - z_T)^2 \quad (20)$$

Subtracting the above equations and taking i =2

$$2d_1 c\tau_{12} + c^2\tau_{12}^2$$
$$= x_2^2 + y_2^2 + z_2^2 - x_1^2 - y_1^2 - z_1^2 - 2(x_2 - x_1)$$
$$\times x_T - 2(y_2 - y_1) y_T - 2(z_2 - z_1) z_T \quad (21)$$

The above equation can be written in matrix form for i = 1, 2, 3 ... M

$$-2 \begin{bmatrix} (x_2 - x_1) & (y_2 - y_1) & (z_2 - z_1) & c\tau_{12} \\ \vdots & \vdots & \vdots & \\ (x_M - x_1) & (y_M - y_1) & (z_M - z_1) & c\tau_{1M} \end{bmatrix} \begin{bmatrix} x_T \\ y_T \\ z_T \\ d_1 \end{bmatrix}$$
$$= \begin{bmatrix} c^2\tau_{12}^2 - x_2^2 - y_2^2 - z_2^2 + x_1^2 + y_1^2 + z_1^2 \\ c^2\tau_{13}^2 - x_3^2 - y_3^2 - z_3^2 + x_1^2 + y_1^2 + z_1^2 \\ \vdots \\ c^2\tau_{1M}^2 - x_M^2 - y_M^2 - z_M^2 + x_1^2 + y_1^2 + z_1^2 \end{bmatrix} \quad (22)$$

$$Ax = b \quad (23)$$

$$\hat{x} = \left(A^H A\right)^{-1} A^H b \quad (24)$$

where:
A = 2× L.H.S matrix.
x = $[x_T, y_T, z_T, d_1]^T$
b = R.H.S matrix

The 3-D coordinates of the target node can be calculated for beacons/sensors greater than 5 (M ≥ 5). In order to improve the accuracy of the algorithm we can increase the number of sensor nodes.

2) TAYLOR SERIES EXPANSION

For sensor nodes less than 5, the Taylor expansion series is implemented to estimate the target node's position [28]. Eq. 20 is linearized for the initial position of the target node $p_{T_0} = [x_{T_0} y_{T_0} z_{T_0}]^T$ through the Taylor series expansion as below:

$$f(x) = f\left(x_{T_0}\right) + \frac{f'\left(x_{T_0}\right)}{1!}\left(x_T - x_{T_0}\right)$$
$$+ \frac{f''(x_{T_0})}{2!}\left(x_T - x_{T_0}\right)^2 + \dots \quad (25)$$

Only the first order for the expansion is kept and the rest is ignored. Hence the positioning equation is as:

$$P_i - f_i\big|_{p_{T_0}} = \frac{\partial f_i}{\partial x_T}\Big|_{p_{T_0}}\left(x_T - x_{T_0}\right) + \frac{\partial f_i}{\partial y_T}\Big|_{p_{T_0}}\left(y_T - y_{T_0}\right)$$
$$+ \frac{\partial f_i}{\partial z_T}\Big|_{p_{T_0}}\left(z_T - z_{T_0}\right) \quad (26)$$

$$\Delta x_T = x_T - x_{T_0} \quad (27)$$
$$\Delta y_T = y_T - y_{T_0} \quad (28)$$
$$\Delta z_T = z_T - z_{T_0} \quad (29)$$

Formulating the Eq. 27, 28 and 29 in matrix form:

$$\begin{bmatrix} P_2 - f_2 \\ P_3 - f_3 \\ \vdots \\ P_M - f_M \end{bmatrix} = \begin{bmatrix} \frac{\partial f_2}{\partial x_T} & \frac{\partial f_2}{\partial y_T} & \frac{\partial f_2}{\partial z_T} \\ \frac{\partial f_3}{\partial x_T} & \frac{\partial f_3}{\partial y_T} & \frac{\partial f_3}{\partial z_T} \\ \vdots & \vdots & \\ \frac{\partial f_M}{\partial x_T} & \frac{\partial f_M}{\partial y_T} & \frac{\partial f_M}{\partial z_T} \end{bmatrix} \begin{bmatrix} \Delta x_T \\ \Delta y_T \\ \Delta z_T \end{bmatrix} \quad (30)$$

$$A\Delta x = P \quad (31)$$

$$\widehat{\Delta x} = \left(A^H A\right)^{-1} A^H P \quad (32)$$

$$\hat{x} = \widehat{\Delta x} + p_{T_0} \quad (33)$$

where: A = L.H.S matrix.

$$\Delta x = [\Delta x_T, \Delta y_T, \Delta z_T]^T$$
$$b = \text{R.H.S differential matrix}$$

V. RESULTS AND ANALYSIS

Using various mathematical models for the channel, the positioning error, and the positioning explained in Sections 3 and 4, the NS-3 based VLC-IPS module is designed and implemented for various error rate models and the propagation loss models. The performance for the VLC module is tested on the basis of BER and Signal-to-Noise-Ratio (SNR) calculation at least under Variable pulse position modulation (VPPM) modulation scheme. The channel parameters, taken as standard values and implemented, are given in Table 1 [3], [4], [42]. The Performance results are given both in analytical and graphical forms for both the LoS and NLoS channel models.

For the positioning scenario, the current testing involves the multilateration combined with RSSI scheme implemented on a Wi-Fi based network. The positioning is calculated using the variance of Log distance Propagation loss model known as Three Log Distance Propagation Loss Model. Four beacon nodes are placed in a single line with the unknown node placed at an initial distance from them. It should be noted that the distance between the beacon nodes is kept constant while the distance between each beacon node and the unknown node is analytically calculated. Hence, the estimated position of the unknown node is calculated through Multi-Lateration equation. Through the pathloss model and mobility model, the exact Position and the RSS of the unknown node is calculated which is compared against the estimated position and positioning error is calculated at each time instance. In this way, a positioning error deviation and PDF is generated and the accuracy of the RSSI scheme is calculated.

A. VLC LoS AND NLoS PERFORMANCE

The graphical results in Fig.5-8 signify the performance of the VLC module for various modulation schemes including

TABLE 1. VLC channel modelling parameters.

Parameter	Value
Transmitter Power, Pt	48.573(dBm)
Lambertian Order Semi angle, $\Phi_{1/2}$	**70°**
Noise bandwidth factor, I_2	0.562
Background current IB	5100−6 A
Field-effect transistor (FET) transconductance (gm)	30 ms
electronic charge, q	1.60217e−19 C
Photodetector Area, A	1.0e−4 m^2
field of view, ψ_{con}	**70°**
Transmitter coordinate	(0.0,0.0,50.0)
Transmitter Azimuth	(0.0)
Transmitter Elevation	(180.0)
Receiver coordinate	(0.0,0.0, dist)
Receiver Azimuth	(0.0)
Receiver Elevation	(0.0)
A	0.85
Bandwidth factor, B	10
lower wavelength, λ_{min}	380nm
upper wavelength, λ_{max}	380nm
Distance, d	50 m
PAM, M	4

FIGURE 6. VPPM BER for LoS channel.

FIGURE 5. BER curves for modulation schemes under VLC link.

FIGURE 7. VPPM SNR curve.

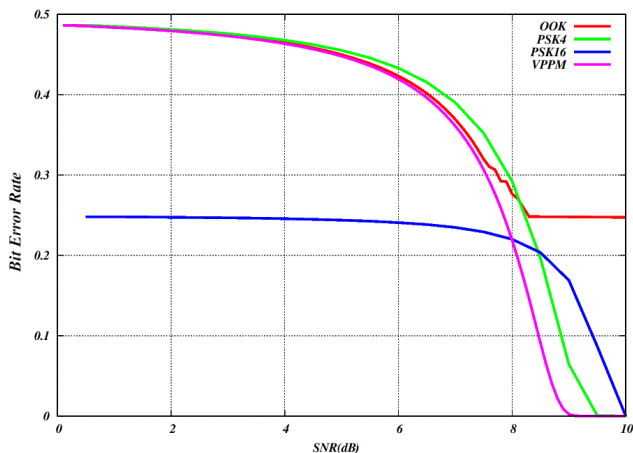**FIGURE 8.** VPPM BER curve for VLC NLoS channel.

OOK, PSK4, PSK16, and VPPM modulation scheme. As Fig. 5 signifies that the performance of VPPM is most efficient hence it is selected to be used in our work for VLC-IPS system. The primary reason for high efficiency lies in the fact that VLC is inherently very good for localization/positioning.

Fig. 6-8 shows the performance of VPPM in terms of BER and SNR measurement for both LoS and NLoS channels, respectively. This scheme comes with illumination with an added feature of dimming control during data communication. As shown in figure, both the operations are performed independently. The VPPM symbols have inverse relations of pulses to the time slots so as the number of empty slots L increases the average power efficiency of VPPM increases
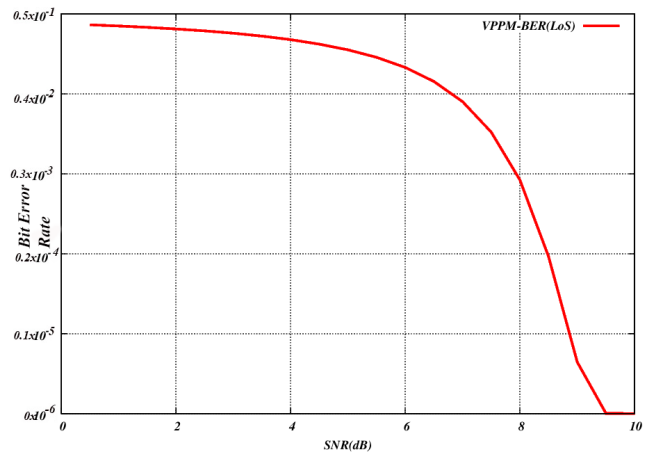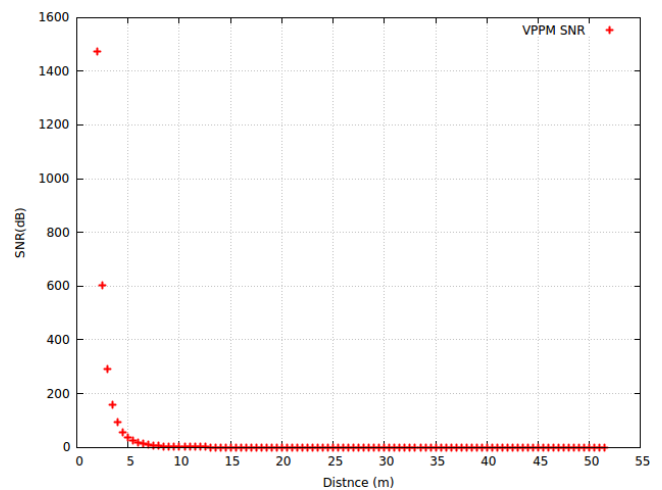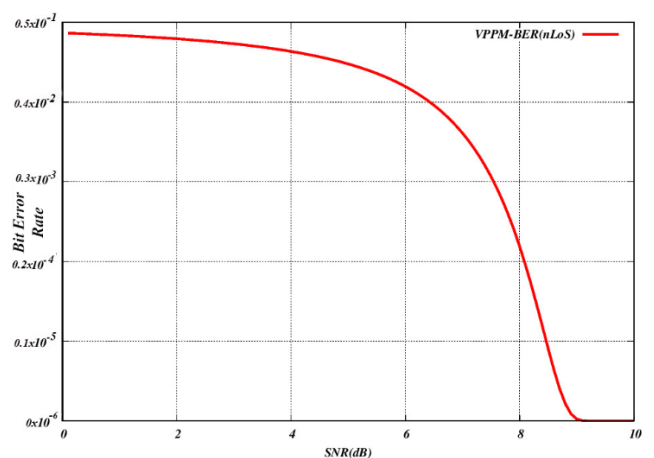
but the bandwidth efficiency decreases. Hence, in VPPM, there is a trade-off between the power and the bandwidth optimization. Since the VPPM works on the time slots and

the pulse positioning, the BER can be computed using Eq. 34.

$$BER = Q\left(\sqrt{\gamma_b} \times \sqrt{\log_2 L}\right) \tag{34}$$

where:

Q refers to Q function
$\gamma_b = \frac{E_b}{N_0} = SNIR$
L = number of time slots

B. RSSI BASED POSITIONING MODEL IMPLEMENTATION FOR WiFi NETWORKS

For RSSI positioning over WiFi channel, the results are obtained in form of graphical, visual, and analytical data compilation and calculation. The graphical results for the received power are plotted taking the standard values as shown in Fig. 9. The WiFi network operating under Three Log Distance Propagation model which is shown visually during their real-time communication as shown in Fig.10. Finally using the receiver power, the position is calculated using the parameters in Table 2 using the trilateration scheme mentioned earlier. The estimated coordinates of unknown node are compared with the actual position to compute the positioning error deviation.
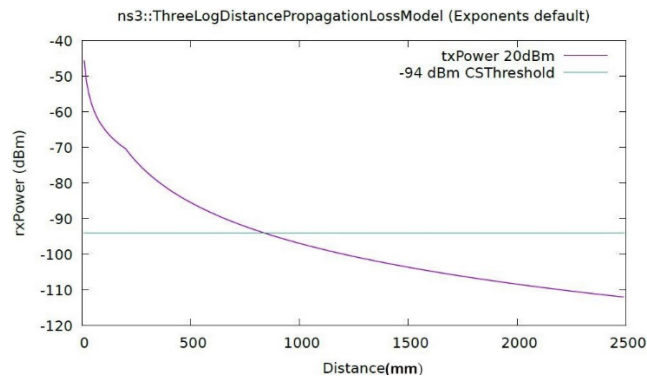

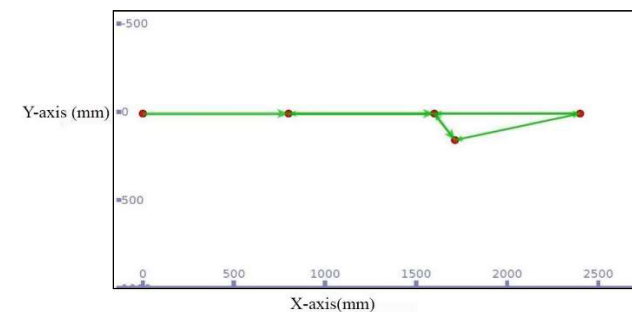**FIGURE 9. Received power for 3logDistance model.**

FIGURE 10. Wi-Fi network under real-time simulation.

The positioning results for a single time instance is provided in Table 3. Using similar calculations, the positioning error deviation, can be calculated at each instance and the

TABLE 2. Positioning model parameters.

Parameter	Value
Number of beacon nodes, Bi	4
Number of unknown nodes, Ui	1
Initial position of beacon node1	(0,0,0)
Distance between each beacon along X-axis (m)	800
Distance between B1 and U, R1	10
Distance between B2 and U, R2	800.06
Distance between B3 and U, R1	1600.03
Distance between B4 and U, R1	2400.02
3log Distance field near, (m)	1.0
3log Distance field, middle (m)	200
3log distance field, far (m)	500
Exponent N_o	1.9
Exponent N_1	3.8
Exponent N_2	3.8

TABLE 3. RSSI based Wi-Fi positioning error results.

Number of anchor nodes	Estimated positioning(m)	Actual Positioning (m)	Mean Positioning Error (m)
4	(X=20, Y=146)	(X=24, Y=160)	∼ 2.2

maximum accuracy can be achieved by calculating the PDF from every positioning error deviation.

C. RSSI BASED POSITIONING MODEL IMPLEMENTATION FOR VLC NETWORK

For RSSI positioning over VLC channel, the channel is designed using equations of NLoS and LoS channel links and the parameters defined in Table 1. The positioning scenario implemented is similar, used for the WiFi-link where four static anchor nodes transmit signals to a random mobile node and the positioning algorithm is implemented at the receiver end.

The pathloss model is implemented is combination of Three Log-Distance Propagation model and Building Propagation Loss Model, which considers the distance loss and real-time features for building obstacles loss like reflection, diffraction, refraction, material density loss, etc., which all contribute to the LoS and NLoS channel attributions for the VLC link. The RSSI is calculated using both the Propagation loss models from all the anchor nodes and using the Multi-Lateration quadratic equations the Estimated position of the mobile node is calculated. The analytical and NetAnim based graphical results are compared with actual position of receiver node and positioning error is calculated. To increase the accuracy of the RSSI based VLC-IPS system, the number of anchor nodes are increased and significant change in positioning error is calculated. Table 4 and Fig. 11 show the results for 4 anchor nodes. Table 5 and Fig. 12 shows result for the 8 anchor nodes for the proposed system.

TABLE 4. RSSI based Wi-Fi positioning error results.

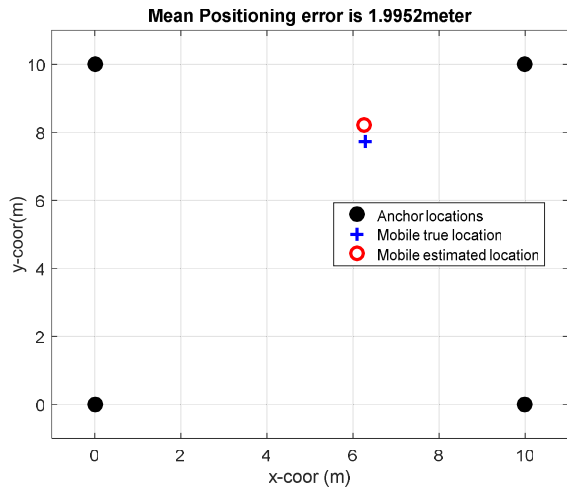| Number of anchor nodes	Estimated positioning(m)	Actual Positioning (m)	Mean Positioning Error (m)
4	(X=38.39, Y=26.02)	(X=39.09, Y=27.72)	~ 1.9

FIGURE 11. VLC-IPS network under real-time simulation for 4 anchor nodes.

TABLE 5. RSSI based Wi-Fi positioning error results.

Number of anchor nodes	Estimated positioning(m)	Actual Positioning (m)	Mean Positioning Error (m)
2	(X=27.692, Y=4.617)	(X=24.181, Y=5.071)	3.50405
4	(X=50.595, Y=69.907)	(X=52.831, Y=69.505)	2.2718
6	(X=43.141, Y=91.064)	(X=42.777, Y=92.395)	1.3792
8	(X= 51.99, Y= 5.382)	(X= 51.587, Y= 6.133)	~ 0.85

D. TDoA BASED POSITIONING MODEL FOR WiFi AND VLC NETWORK

For TDoA positioning, the NS-3 setup provides a comparative analysis for the TDoA based positioning algorithm for both WiFi and VLC based Adhoc network. As discussed in Section IV-B, the TDoA based algorithm uses the time difference of arrival of the transmitted signal from various beacon nodes targeted at the unknown node. The time difference gives rise to phase change which can be represented by the hyperbolas for each sensor and the intersection of these hyperbolas provides the estimation for the location of the target node.

The TDoA algorithm is performed under the assumption that the beacon nodes are stationary and their clocks are well synchronized. This results in zero Doppler Shift effect which means that the TDoA can be estimated by computing the cross correlation between the signals transmitted by all the
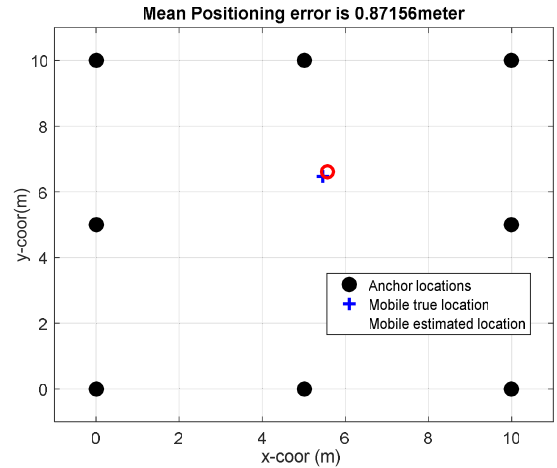

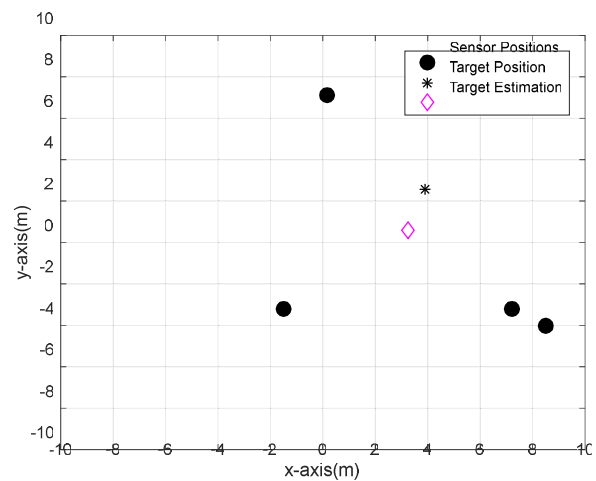**FIGURE 12.** VLC-IPS network under real-time simulation for 8 anchor nodes.

FIGURE 13. TDoA based Wi-Fi network for 4 anchor nodes.

sensors. Once the cross correlation is computed, the TDoA based positioning is estimated through the Least Square Linearization for sensors less than or equal to 4 ($M \leq 4$) and Taylor expansion series for greater than or equal to 5 ($M \geq 5$).

The results obtained in Fig. 13 & 14, are for both WiFi and VLC based networks tested with different number of sensor/beacon nodes to increase the accuracy of the system. It is evident that as the number of sensors/beacon nodes are increased for the VLC network, the accuracy is increased
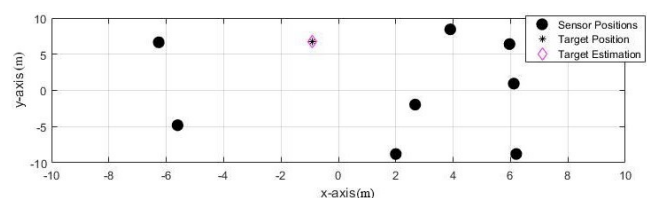

FIGURE 14. TDoA based Wi-Fi network for 8 anchor nodes.

TABLE 6. Positioning error results for TDoA based VLC network.

Scheme	Physical Link	Number of anchor nodes	Estimated positioning(m)	Actual Positioning (m)	Mean Positioning Error (m)
RSSI	WiFi	4	(X=20, y=146)	(X=24, Y=160)	~ 2.2
	VLC	2	(X=27.692, Y=4.617)	(X=24.181, Y=5.071)	3.50405
		4	(X=50.595, Y=69.907)	(X=52.831, Y=69.505)	2.2718
		6	(X=43.141, Y=91.064)	(X=42.777, Y=92.395)	1.3792
		8	(X= 51.99, Y= 5.382)	(X= 51.587, Y= 6.133)	~ 0.85
TDoA	WiFi	4	(X=2.198, Y=5.773)	(X=3.2619, Y=4.4887)	~ 0.2842
	VLC	4	(X=0.0417, Y=0.2925)	(X=0.0732, Y=0.0850)	~ 0.005
		6	(X=3.651, Y=1.296)	(X=3.657, Y=1.302)	~ 0.0002
		8	(X=0.920, Y=6.778)	(X=0.923, Y=6.771)	~8e-5

exponentially. The VLC network implemented is for both LoS and NLoS channel combined specifically for 8 beacons network. In the following experiment the positioning of the beacon and target nodes are randomized to provide a more realistic simulation and all the real-time parameters of an indoor network are incorporated. The Results of the simulation are obtained using NetAnim and analytical data is collected accordingly.

VI. CONCLUSION

In this work, we have successfully carried out localization comparison of TDoA and RSSI schemes under WiFi and VLC channels in real-time environment. The inclusion of VLC module in NS-3 library has made significant contribution and now VLC channel can be used for different application. The TDoA based VLC scheme outperforms other existing schemes owing to the fact that the VLC gives superior positioning accuracy due to its unique channel characteristics.

The VLC based Ad hoc Networks are the future of wireless networking and data communication. With its vast applications and salient features VLC technology will be contributing for exponential technological advancements in all the domains. VLC based positioning systems are going to be highly essential in the coming age of autonomous network systems and smart city concept. Since the testbeds for these technologies are quite expensive, the real-time discrete event network simulators like NS-3 provides the most suitable alternatives for the testing of the network performance and feasibility and simulation purposes.

REFERENCES

[1] A. Goldsmith, *Wireless Communications*, London, U.K.: Cambridge Univ., 2005.

[2] A. Calisti, "Simulation of visible light communication for vehicular networks," M.S. thesis, Dept. Eng. Archit., Univ. Bologna, Bologna, Italy, 2014.

[3] Z. Ghassemlooy, "Optical wireless communication," in *System and Channel Modelling with MATLAB*. Boca Raton, FL, USA: CRC Press, 2012.

[4] S. M. Sheikh, H. R. Ali, H. M. Asif, S. Baig, and A. A. Khan, "Design of NS3 VLC module and performance analysis of ad hoc network under VLC and Wi-Fi layers," *Int. J. Commun. Syst.*, vol. 31, no. 14, p. e3764, Sep. 2018.

[5] T. Jerkovits, G. Liva, and A. G. I. Amat, "Improving the decoding threshold of tailbiting spatially coupled LDPC codes by energy shaping," *IEEE Commun. Lett.*, vol. 22, no. 4, pp. 660–663, Apr. 2018.

[6] Y. Fang, P. Chen, G. Cai, F. C. M. Lau, S. C. Liew, and G. Han, "Outage-limit-approaching channel coding for future wireless communications: Root-protograph low-density parity-check codes," *IEEE Veh. Technol. Mag.*, vol. 14, no. 2, pp. 85–93, Jun. 2019.

[7] A. Khalid and H. M. Asif, "OCDMA and OSTBC based VLC transceiver design using NI cDAQ," *Photonic Netw. Commun.*, vol. 35, no. 1, pp. 97–108, Feb. 2018.

[8] A. Naz, "Tri-lateration based indoor positioning system for VLC," M.S. thesis, COMSATS Inst. Inf. Technol., Lahore, Pakistan, 2017.

[9] A. Naz, H. M. Asif, T. Umer, and B.-S. Kim, "PDOA based indoor positioning using visible light communication," *IEEE Access*, vol. 6, pp. 7557–7564, 2018.

[10] Y. Wang, X. Yang, Y. Zhao, Y. Liu, and L. Cuthbert, "Bluetooth positioning using RSSI and triangulation methods," in *Proc. IEEE 10th Consum. Commun. Netw. Conf. (CCNC)*, Jan. 2013, pp. 837–842.

[11] A. Ren, F. Zhou, A. Rahman, X. Wang, N. Zhao, and X. Yang, "A study of indoor positioning based on UWB base-station configurations," in *Proc. IEEE 2nd Adv. Inf. Technol., Electron. Automat. Control Conf. (IAEAC)*, Mar. 2017, pp. 1939–1943.

[12] B. Jachimczyk, D. Dziak, and W. J. Kulesza, "RFID—Hybrid scene analysis-neural network system for 3D indoor positioning optimal system arrangement approach," in *Proc. IEEE Int. Instrum. Meas. Technol. Conf. (IMTC)*, Montevideo, Uruguay, May 2014, pp. 191–196.

[13] S. S. Saab and Z. S. Nakad, "A standalone RFID indoor positioning system using passive tags," *IEEE Trans. Ind. Electron.*, vol. 58, no. 5, pp. 1961–1970, May 2011.

[14] C. Wu, Q. Mu, Z. Zhang, Y. Jin, Z. Wang, and G. Shi, "Indoor positioning system based on inertial MEMS sensors: Design and realization," in *Proc. IEEE Int. Conf. Cyber Technol. Automat., Control, Intell. Syst. (CYBER)*, Jun. 2016, pp. 370–375.

[15] Y. Tian, D. Shigaki, W. Wang, and C.-J. Ahn, "A weighted least-squares method using received signal strength measurements for WLAN indoor positioning system," in *Proc. 20th Int. Symp. Wireless Pers. Multimedia Commun. (WPMC)*, Dec. 2017, pp. 310–314.

[16] J. Kim and H. Jun, "Vision-based location positioning using augmented reality for indoor navigation," *IEEE Trans. Consum. Electron.*, vol. 54, no. 3, pp. 954–962, Aug. 2008.

[17] V. Pasku, A. D. Angelis, M. Dionigi, G. D. Angelis, A. Moschitta, and P. Carbone, "A positioning system based on low-frequency magnetic fields," *IEEE Trans. Ind. Electron.*, vol. 63, no. 4, pp. 2457–2468, Nov. 2016.

[18] J. Qi and G.-P. Liu, "A robust high-accuracy ultrasound indoor positioning system based on a wireless sensor network," *Sensors*, vol. 17, no. 11, p. 2554, Nov. 2017.

[19] A. Khalid, T. Umer, M. K. Afzal, S. Anjum, A. Sohail, and H. M. Asif, "Autonomous data driven surveillance and rectification system using in-vehicle sensors for intelligent transportation systems (ITS)," *Comput. Netw.*, vol. 139, pp. 109–118, Jul. 2018.

[20] H. Dai, H.-B. Liu, X.-S. Xing, and Y. Jin, "Indoor positioning algorithm based on parallel multilayer neural network," in *Proc. Int. Conf. Inf. Syst. Artif. Intell. (ISAI)*, Jun. 2016, pp. 356–360.

[21] P. Davidson and R. Piche, "A survey of selected indoor positioning methods for smartphones," *IEEE Commun. Surveys Tuts.*, vol. 19, no. 2, pp. 1347–1370, 2nd Quart., 2017.

[22] T. Raharijaona, R. Mawonou, T. V. Nguyen, F. Colonnier, M. Boyron, J. Diperi, and S. Viollet, "Local positioning system using flickering infrared LEDs," *Sensors*, vol. 17, no. 11, p. 2518, Nov. 2017.

[23] C. Randell and H. Muller, "Low cost indoor positioning system," in *Proc. Int. Conf. Ubiquitous Comput.*, London, U.K., Sep. 2001, pp. 42–48.

[24] Y. Fukuju, M. Minami, H. Morikawa, and T. Aoyama, "DOLPHIN: An autonomous indoor positioning system in ubiquitous computing environment," in *Proc. IEEE Workshop Softw. Technol. Future Embedded Syst. (WSTFES)*, Hokkaido, Japan, May 2003, pp. 53–56.

[25] G. Li, E. Geng, Z. Ye, Y. Xu, and H. Zhu, "An indoor positioning algorithm based on RSSI real-time correction," in *Proc. 14th IEEE Int. Conf. Signal Process. (ICSP)*, Chongquing, China, Aug. 2018, pp. 129–133.

[26] S. Ali-Loytty, T. Perala, V. Honkavirta, and R. Piche, "Fingerprint Kalman filter in indoor positioning applications," in *Proc. IEEE Int. Conf. Control Appl.*, Jul. 2009, pp. 1678–1683.

[27] A. Kotanen, M. Hannikainen, H. Leppakoski, and T. D. Hamalainen, "Experiments on local positioning with bluetooth," in *Proc. Int. Conf. Inf. Technol., Coding Comput. (ITCC)*, Apr. 2003, pp. 297–303.

[28] X.-W. Shi and H.-Q. Zhang, "Research on indoor location technology based on back propagation neural network and Taylor series," in *Proc. 24th Chin. Control Decis. Conf. (CCDC)*, May 2012, pp. 1886–1890.

[29] H. Zhang, J. Cui, L. Feng, A. Yang, H. Lv, B. Lin, and H. Huang, "High-precision indoor visible light positioning using deep neural network based on the Bayesian regularization with sparse training point," *IEEE Photon. J.*, vol. 11, no. 3, pp. 1–10, Jun. 2019.

[30] P. Du, S. Zhang, C. Chen, A. Alphones, and W.-D. Zhong, "Demonstration of a low-complexity indoor visible light positioning system using an enhanced TDOA scheme," *IEEE Photon. J.*, vol. 10, no. 4, pp. 1–10, Aug. 2018.

[31] A. Arafa, X. Jin, D. Guerrero, R. Klukas, and J. F. Holzman, "Imaging sensors for optical wireless location technology," in *Proc. Int. Tech. Meeting Satellite Division Inst. Navigat.*, Sep. 2013, pp. 1020–1023.

[32] M. S. Rahman, M. M. Haque, and K.-D. Kim, "Indoor positioning by LED visible light communication and image sensors," *Int. J. Electr. Comput. Eng.*, vol. 1, no. 2, pp. 161–170, Nov. 2011.

[33] U. Nadeem, N. U. Hassan, M. A. Pasha, and C. Yuen, "Highly accurate 3D wireless indoor positioning system using white LED lights," *Electron. Lett.*, vol. 50, no. 11, pp. 828–830, May 2014.

[34] H.-S. Kim, D.-R. Kim, S.-H. Yang, Y.-H. Son, and S.-K. Han, "An indoor visible light communication positioning system using a RF carrier allocation technique," *J. Lightw. Technol.*, vol. 31, no. 1, pp. 134–144, Jan. 1, 2013.

[35] A. Naz, H. M. Asif, T. Umer, S. Ayub, and F. Al-Turjman, "Trilateration-based indoor localization engineering technique for visible light communication system," *Softw., Pract. Exper.*, vol. 53, no. 3, pp. 503–516, 2021.

[36] A. Naz, N. U. Hassan, M. A. Pasha, H. Asif, T. M. Jadoon, and C. Yuen, "Single LED ceiling lamp based indoor positioning system," in *Proc. IEEE 4th World Forum Internet Things (WF-IoT)*, Feb. 2018, pp. 682–687.

[37] J. Etter-Olguín, C. Duran-Faundez, J. Rohten, R. Seguel-Cardenas, and I. Santana, "Simulation of RSSI-based positioning algorithms for wireless network using ns−3," in *Proc. Conf. Sci. Int. (CCI)*, Santiago, Chile, 2019.

[38] Y. Li, X. He, and S. Liu, "Wireless localization algorithm based on path loss model parameter estimated in real-time," *Chin. J. Sens. Actuators*, vol. 23, no. 9, pp. 1328–1333, 2010.

[39] M. Ahsan and H. M. Asif, "ESIM-OFDM-based transceiver design of a visible light communication system," *Int. J. Commun. Syst.*, vol. 30, no. 8, p. e3175, May 2017.

[40] C. Chen, D. Basnayaka, and H. Haas, "Non-line-of-sight channel impulse response characterization in visible light communication," in *Proc. IEEE Int. Conf. Commun. (ICC)*, May 2016, pp. 1–6.

[41] A. U. Rehman, "A performance comparison of network simulators for wireless networks," in *Proc. IEEE Int. Conf. Control Syst., Comput. Eng.*, Penang, Malaysia, 2012, pp. 34–38.

[42] A. Aldalbahi, M. Rahaim, A. Khreishah, M. Ayyash, R. Ackerman, J. Basuino, W. Berreta, and T. D. C. Little, "Extending ns−3 to simulate visible light communication at network level," in *Proc. 23rd Int. Conf. Telecommun. (ICT)*, Thessaloniki, Greece, 2016, pp. 1–6.

• • •